APRIL-mediated anti-inflammatory response of astrocytes in multiple sclerosis

Running head: a protective role for APRIL in MS

Authors:

L. Baert[1*], M. Benkhoucha[2*], N. Popa[3], M.C. Ahmed[1], B. Manfroi[1], J. Boutonnat[4], N. Sturm[4], G. Raguenez[3], M. Tessier[3], O. Casez[5], R. Marignier[6], M. Ahmadi[7], A. Broisat[7], C. Ghezzi[7], C. Rivat[8], C. Sonrier[8], M. Hahne[9], D. Baeten[10,11], R.R. Vives[12], H. Lortat-Jacob[12], P.N. Marche[1], P. Schneider[13], H.P. Lassmann[14], J. Boucraut[3], P. Lalive[2*], B. Huard[1*, **]

Affiliations:

[1]Institute for advanced biosciences, University Grenoble-Alpes/INSERM U1209/CNRS UMR5309, La Tronche, France.
[2] Department of Pathology and Immunology, School of Medicine, Geneva University, Switzerland.
[3] CRN2M, CNRS UMR 6231, Méditerranée University, Medicine Faculty, Marseille, France.
[4] Department of anatomopathology and cytology, University Hospital, Grenoble, France.
[5] Neurology, Grenoble University hospital, La Tronche, France.
[6] Faculty of Medicine Laennec, Lyon Neurosciences Research Centre, Neuro-inflammation and Neuro-oncology Team, Lyon, France.
[7] Radiopharmaceutiques Biocliniques, INSERM U1309, Grenoble, France
[8] Neurosciences Institute, INSERM U1051, Montpellier, France
[9] Institute for molecular genetics, CNRS UMR5535, Montpellier, France.
[10] Department of Clinical Immunology & Rheumatology, Academic Medical Center, University of Amsterdam, The Netherlands.
[11] Department of Experimental Immunology, Academic Medical Center, University of Amsterdam, Amsterdam, The Netherlands.
[12] Institute of structural biology, University Grenoble-Alpes, UMR5075, CNRS-CEA
[13] Department of Biochemistry, University of Lausanne, Epalinges, Switzerland.
[14] Center for Brain Research, Medical University of Vienna, Vienna, Austria

***** equal contribution
****** Corresponding author:

Bertrand Huard
Bertrand.huard@univ-grenoble-alpes.fr

Word count:
Abstract: 232
Introduction: 251
Discussion: 756
Body text: 3897
Figures (color): 7 (2)
Table: 1

Abstract:

Objective: the two related TNF members APRIL and BAFF are currently targeted in autoimmune diseases as B-cell regulators. In multiple sclerosis (MS), combined APRIL/BAFF blockade led to an unexpected exacerbated inflammation in the central nervous system (CNS) of patients. Here, we investigate the role of the APRIL/BAFF axis in the CNS.

Methods: APRIL expression was analyzed in MS lesions by immunohistochemistry. The *in vivo* role of APRIL was assessed in the murine MS model, experimental autoimmune encephalitis (EAE). Functional *in vitro* studies were performed with human and mouse astrocytes.

Results: APRIL was expressed in lesions from EAE. In its absence, the disease was worst. Lesions from MS patients also showed APRIL expression upon infiltration of macrophages. Notably, all the APRIL secreted by these macrophages specifically targeted astrocytes. The upregulation of chondroitin sulfate proteoglycan (CSPG) bearing sometimes chondroitin sulfate of type E sugar moieties, binding APRIL, in reactive astrocytes explained the latter selectivity. Astrocytes responded to APRIL by producing sufficient amount of IL-10 to dampen antigen-specific T-cell proliferation and pathogenic cytokine secretion. Finally, an intraspinal delivery of recombinant APRIL before disease onset shortly reduced EAE symptoms. Repeated intravenous injections of recombinant APRIL before and even at disease onset had also an effect.

Interpretation: our data show that APRIL mediates an anti-inflammatory response from astrocytes in MS lesions. This protective activity is not shared with BAFF.

Introduction

B cells are currently targeted in autoimmune diseases, and atacicept is one drug targeting B cells [1]. The clinical trial testing atacicept in multiple sclerosis (ATAMS) has provoked an unexpected exacerbation of inflammation in the central nervous system (CNS) of treated patients, halting the trial [2]. Atacicept is an immunoglobulin-fused soluble form of the transmembrane activator and CAML interactor (TACI, TNFRSF13b), a receptor belonging to the TNF receptor superfamily. TACI binds two related members of the TNF ligand superfamily, the B cell activation factor from the TNF family (BAFF, TNFSF13b) and a proliferation inducing ligand (APRIL, TNFSF13) [3]. Atacicept mediated progression of a neurodegenerative disease has been reproduced with the ATON trial, testing atacicept in optic neuritis (ON) [4]. Concurrently, atacicept-mediated worsening was also reported in a variant of experimental autoimmune encephalitis (EAE) conducting to ON in rat [5]. These results may mean that antagonism of the APRIL/BAFF axis accelerates autoimmune neurodegeneration.

BAFF and APRIL play a non-redundant role in humoral immunity [6]. APRIL mainly acts on antibody-producing plasma cells (PC) by driving isotype switch and survival. In addition to TACI, BAFF and APRIL also share the B cell maturation antigen (BCMA) as receptor [3]. To efficiently signal in TACI/BCMA expressing target cells, APRIL needs heparan sulfate proteoglycans (HSPG) as coreceptors [7,8]. BAFF does not share this coreceptor binding activity, but has a specific receptor, BAFF-R [9]. In the present study, we are showing that APRIL, but not BAFF, may have a protective role in the CNS by acting on astrocytes.

Material and Methods

Human samples and mouse preclinical model.

The human autopsies from MS patients have been previously described [10]. Control brain autopsies were obtained in healthy white matter area from a patient suffering from sclerosis lateral amyotrophic, and three patients deceased from non-neurodegenerative disorders. The *APRIL* KO mice used were the one originally described by varfolomeev et al., [11]. Controls were wild type mice housed in the same conditions. EAE was induced in female mice with a commercial emulsion with 30 µg of myelin oligodendrocyte glycoprotein 35–55 peptide in complete Freund adjuvant, followed 24 h later by an i.v. injection of 100 ng of pertussis toxin (Hooke Laboratories). Mice were scored as follows: 0, no symptoms; 1, decreased tail tone; 2, mild monoparesis or paraparesis; 3, severe paraparesis; 4, paraplegia and/or quadriparesis; and 5, moribund condition or death. Intraspinal injections were performed into the spinal subarachnoidal space at the L5-L6 level using a 30-gauge needle (BD Micro-fine). The correct delivery was systematically checked by the mouse tail flick reflex. I.v. injections were performed in the tail vein. Disease scoring was conducted in a randomized manner by two independent investigators masked to the mouse genotype and experimental group. All experimentation was prepared in concordance with the ARRIVE guidelines, and was approved by the Grenoble ethical committee.

Immunohistochemistry

Luxol fast blue (Sigma) was used to stain myelin. Formalin-fixed paraffin-embedded biopsies were stained with Stalk-1 (rabbit polyclonal) and Aprily-8 (mouse IgG1) detecting APRIL-producing cells and secreted APRIL, respectively, as previously described [12]. The anti-CD68 (clone PGM1, IgG3, Dako) was used at 10 µg/ml after heat induced epitope retrieval (HIER) in Tris 10 mM EDTA 1 mM, pH 9. The polyclonal anti-NADPH oxydase

has been described elsewhere [10].The anti-CSPG (CS56, IgM) was from Sigma, and used at 10 µg/ml without HIER. The anti-HSPG 3g10 (IgG2b) and 10e4 (IgM) were from Euromedex, and used at 10µg/ml. 10e4 recognizes native HSPG, while 3g10 recognizes HSPG after heparinase digestion [13]. The ScFv anti-CSE, GD3G7, was a kind gift of Dr Th. van Kuppevelt (Nijmegen, The Netherlands). GD3G7 binding was revealed by a polyclonal anti-VSV tag (Abcam). Detection was based on a horseradish-peroxidase (HRP)-labelled polymer conjugated with secondary antibodies (Dako, EnVision®+ System-HRP kit). Development was made using 3-amino-9-ethyl-carbazol substrate (Sigma-Aldrich) and counterstain with Mayer's hematoxylin (Dako). For multicolor immunofluorescence stainings, the following primary antibodies were used: Stalk-1, Aprily-8, 3g10, 10e4, CS-56, 3g10, GD3G7, anti-CD68, anti-GFAP (polyclonal rabbit IgG, 1/500, Dako). Detection was performed with anti-VSV-FITC, and alexa-488, PE, alexa-350 conjugated anti-Ig secondary reagents. DAPI (Dako) was used for nucleus staining. Stainings were visualised with an Olympus BX-41 microscope (Zeiss).

Recombinant protein production

Expression constructs for Fc-tagged muAPRIL$_{A88}$ (88-233), muAPRIL$_{H98}$ (98-233), and muBAFF (134-285) have been described elsewhere [8]. Fc-tagged human glucocorticoid-induced TNF-related ligand (Fc-hGITRL (47-177)) was used as negative control. Due to the T-cell activation property of GITR-L, Fc-tagged EDA (Fc-hEDA (245-391) was used in the T-cell *in vitro* stimulation assay and in the *in vivo* treatment assay. Recombinant proteins were transiently produced in 293T HEK cells with serum-free Optimem 1 medium. Purification was performed with Protein-A Sepharose (GE Healthcare). The absence of endotoxin contamination was assessed with the limulus amebocyte lysate kit (Enzo Life Sciences).

Radioimaging

Proteins were radiolabelled with Iodogen, and injected i.v. (3.7MBq/mouse, 6 mice/group). 48h later, the animals were euthanized, perfused with saline, and the activity in the spinal cord expressed as a percent injected dose per gram (%ID/g).

Brain cell culture

Human astrocytes were purchased from Sciencell Research Laboratories. The astrocytoma cell line CRT was purchased from American Tissue Culture Collection. Primary mixed glial cultures were established from the forebrains of C57Bl/6J newborn mice. Amoeboid microglia floating cells were detached from the astroglial monolayer by manual shaking. The remaining adherent monolayer contained astrocytes and adherent microglia. The cells were detached with trypsin. The microglia was removed by adhesion on plastic during 30 minutes. LPS and Poly-IC were from Sigma. For the endocytosis experiment, the CRT cell line was incubated with 1 µg/ml of human FLAG-tagged APRIL for 30 mn at 4°C, washed and further incubated at either 4°C or 37°C for 45 minutes. Cells were then fixed in PFA 4% followed by quenching in PBS glycine 0.1M. Astrocytes bound APRIL was detected with a biotinylated anti-FLAG antibody (1µg/ml, Sigma) and PE-conjugated streptavidin (BD biosciences) in PBS 2% BSA 0.2% saponin. Cholera toxin B subunit FITC (10µg/ml, Sigma) and DAPI (5µg/ml) were used to label plasma membrane and nucleus, respectively. Cells were analyzed on a LSM510 confocal microscope (Carl Zeiss) with a plan-Apochromat 63x/1,4 oil objective.

Flow cytometry

Cells were incubated for 30 mn on ice with Fc-APRIL$_{A88,}$ Fc-APRIL$_{H98}$ or Fc-GITRL, each at 10 µg/ml. PE-conjugated anti-IgG secondary antibody was used to detect the binding. The 10e4 and CS-56 mAbs were also used at 10 µg/ml, followed by FITC-conjugated goat

anti-mouse IgM. Heparinase, chondroitinase and NaClO3 treatments were performed as previously described [14]. 7AAD (BD biosciences) was used at 50 µg/ml to exclude dead cells. Cytometry bead arrays (CBA) for mouse cytokines were from Becton Dickinson. Fluorescence was analyzed by flow cytometry on an Accuri C6 apparatus (BD Biosciences).

For the analysis of spinal cord cells, mice were first perfused with saline and infiltrating cells and microglia were obtained at the interphase between the 75% and 35% Percoll fractions, and washed with HBSS 3% FCS. Cells were stained with fluorochrome-conjugated CD45, CD11b, MHC-II (I-Ab), CX3CR-1 and Ly6C from BD Biosciences, and sorted on a FACSAria III cell sorter (BD Biosciences).

Surface plasmon resonance

SPR analyses were performed on a BIAcore 3000 (GE). Binding assays on glycosaminoglycan (GAG) surfaces were performed as previously described [15]. Trimeric human FLAG-tagged $APRIL_{A88}$ was used [8]. Data were analyzed using the BIAeval 3.1 software.

***In vitro* T-cell activation assays**

2D2 TCR transgenic mice were obtained from Charles River. After red blood cell lysis, spleen cells from 2D2 mice were stimulated with the MOG 35-55 peptide (3 µg/ml, polypeptide). Semi-confluent mouse primary astrocytes were prestimulated for 48 hours with Fc-$APRIL_{A88}$ at 10 µg/ml. T-cell proliferation was assessed after standard CFSE labeling and flow cytometry analysis (LSR-II, Becton Dickinson). Cytokine secretion was assessed by ELISA in the supernatant three days after stimulation. The rat anti-mouse IL-10 (clone JES5-2a5, Biolegend) was used at 10 µg/ml.

RT-PCR

Total RNA extractions were performed with the RNeasy Mini Kit (QIAGEN). The reverse transcription was performed with M-MLV reverse transcriptase (Invitrogen) and random primers. The following 5' to 3' forward GTGAATATTTTGACAGTCTGCT and reverse ATCTAGTGTGAGTTGGCTTC for muBCMA, forward CCAAAGATCAGTACTGGGAC and reverse AAGCTACACGTTTCCACAG for muTACI, forward GGGCAGTGCTCCCAAAAT and reverse TCGTTTTCGTGGTGACAAGA for huBCMA,. PCR was performed using Taq Platinium polymerase kit (thermofisher). The amplification procedure included a 3 min step at 94°C followed by 35 cycles with 30 sec at 94°C as denaturation step, 30 sec at 55°C as hybridization step, and 1 min at 72°C as elongation step. A final 4 min at 72°C step was used for final elongation. PCR products were visualized on 1% agarose gel using Gelgreen (Ozyme) dye under UV illumination. Quantitative PCR (qPCR) was performed on a 7500 Real Time PCR System with Power Syber Green (Applied Biosystem). The following CTGGAGGCCAGGGAGACAT and reverse GCACGGTCAGGATCAGAAGG for muAPRIL, forward AGCATGGCCCAGAAATCAAGGA and reverse GCCTTGTAGACACCTTGGTCTTG for muIL-10, forward TTGTCAAGCTCATTTCCTGGTATG and reverse GGATAGGGCCTCTCTTGCTCA for muGAPH were used.

Statistics

EAE was analyzed by a using a Mann-Whitney U-test either day by day or for the entire course of the experiment. QPCR results were analyzed by an ANOVA-based test with a Tukey's multiple comparison. P values inferior to 0.05 were considered statistically significant. ELISA and proliferation were analyzed by using parametric unpaired T-test.

Results

Exacerbated EAE in the absence of APRIL

To unveil the putative role of APRIL in MS, we first compared EAE in WT and *APRIL* KO mice. Figure 1A shows an exacerbated EAE starting around disease peak. In the periphery of EAE mice, we did not detect any difference in the level of disease inducing IFN-γ and IL-17A cytokines measured after *in vitro* restimulation of spleen and draining lymph node cells with the MOG priming peptide (figure 1B). Regarding APRIL expression in mouse spinal cord, we observed a strong upregulation of APRIL transcripts also around disease peak that went back down to control levels afterwards (figure 1C). In fact, the expression profile of APRIL mRNA was highly similar to that of MHC class II, a marker of CNS inflammation commonly used in EAE. The myeloid lineage is the major source of APRIL [16]. In EAE, infiltrating macrophages joins the pool of brain resident myeloid microglial cells. We examined APRIL expression in these two myeloid subsets. APRIL mRNA was barely detectable in $Ly6C^{-}CX3CR1^{+}CD11b^{+}CD45^{int}$ microglial cells from naive mice (figure 1D). During EAE, activated microglia cells defined by MHC class II expression slightly upregulated APRIL expression, while $Ly6C^{+}CX3CR1^{int}CD11b^{+}CD45^{high}$ CNS-infiltrating macrophages were an abundant source of APRIL. These results demonstrated that upregulation of APRIL occurs during EAE in mouse CNS, and identified infiltrating macrophages as the major source of APRIL in EAE. In the absence of APRIL, the disease is exacerbated. We observed this exacerbation without a concomitant enhanced T-cell priming in the periphery, strongly suggesting a local role for APRIL in the CNS.

APRIL expression in MS lesions

We next studied APRIL expression in MS patients, and also observed a strong expression of APRIL *in situ*. In chronic active lesions, which are characterized by a dense rim

of activated macrophages at the active lesion edge and a diffuse infiltration of macrophages with late myelin degradation products in the lesion center, immunohistochemical studies revealed a subset of macrophages producing APRIL at the active edge (figure 2A). There, we did not detect full-length APRIL, theoretically detectable with our pair of antibodies by a colocalization of APRIL production and secreted APRIL in producing cells, as in all the other human tissues analyzed so far. Rather, most if not all of the secreted APRIL localized throughout the entire lesion and in part also in the surrounding peri-plaque white matter. APRIL production was different according to disease stages and lesion types as defined previously [17]. Fulminant acute lesions are present in patients with acute MS (AMS) and relapse/remitting MS (RRMS) [18]. In these lesions, active demyelination is predominantly associated with microglia activation, expressing high levels of NADPH oxidase, and macrophages in the lesions, which contain myelin degradation products [19]. There, APRIL production was low and restricted to some scattered macrophages in the lesions and in the perivascular space (figure 2B). There was no evidence for APRIL production by activated microglial cells dominating such lesions. The typical feature of slowly expanding lesions from patients with primary or secondary progressive MS (PPMS, SPMS) is the presence of a rim of $CD68^+$ activated microglia with some scattered macrophages, which contain early myelin degradation products. In these lesions, the APRIL-producing cells concerned only a subset of the total $CD68^+$ population (figure 2C). In inactive lesions, APRIL production was sparse or absent (data not shown). In most cases, we also observed APRIL-production in granulocytes within blood vessel lumina (see top insert figure 2B) and occasionally present within the pathological tissue. Regarding secreted APRIL, it was found in every single active plaque (acute/chronic active plaques and slowly expanding lesions), accumulating in cells with a morphology reminiscent of astrocytes (see inserts bottom right panels), but only rarely in astrocytes from inactive lesions. No reactivity for APRIL production and secreted APRIL

was detected in the normal appearing white matter (NAWM) of these patients, defined as a zone at least one centimeter distal from the lesion edge. We did not detect APRIL production and secreted APRIL in the white matter from control brain autopsies (figure 2D). Table 1 summarizes the pattern of APRIL production and secreted APRIL observed in all MS patients analyzed. Costaining experiments confirmed that a subset of $CD68^+$ myeloid cells produced APRIL, and that secreted APRIL bound to $GFAP^+$ astrocytes (figure 2E). The apparent intracellular localization of APRIL in astrocytes indicated a potential *in situ* internalization of APRIL that we demonstrated *in vitro* upon incubation of astrocytes with recombinant soluble APRIL at 37°C (figure 2F). We used two recombinant soluble forms of APRIL, $APRIL_{A88}$ and $APRIL_{H98}$. $APRIL_{A88}$ has the potential to bind the signaling receptors TACI, BCMA and the coreceptor HSPG. On the contrary, $APRIL_{H98}$ binds only TACI and BCMA because of the deletion of the HSPG-binding site. In this experiment, $APRIL_{A88}$ internalization was a rapid process, detectable as early as 5 mn after incubation at 37°C, and internalized APRIL was quite stable, since we did no detect degradation within a time frame of 45 mn at 37°C. By contrast, $APRIL_{H98}$ did not get internalized. We did not detect APRIL mRNA by qPCR in resting mouse primary astrocytes, even upon activation by the Toll-like receptor (TLR) ligands LPS and Poly-IC (data not shown). Taken together, our *in situ* analysis shows that a subset of macrophages infiltrating lesions from MS patients produces APRIL, and the secreted product accumulates into astrocytes.

CS of type E from astrocytes is a new binding partner for APRIL in MS lesions

We next analyzed expression of APRIL receptors on astrocytes. $APRIL_{A88}$ and to a lesser extent $APRIL_{H98}$ bound to the control multiple myeloma (MM) cell line L363, expressing the HSPG CD138 (also known as syndecan-1) as well as TACI and BCMA (figure 3A). Human/mouse primary astrocytes and the astrocytoma cell line CRT bound only

$APRIL_{A88}$, excluding surface expression of TACI and BCMA on primary astrocytes. As another control, BAFF did not bind to these astrocytes (data not show). RT-PCR analysis for TACI and BCMA mRNA further excluded a putative intracellular location of these two receptors (figure 3B). Human primary astrocytes and the CRT astrocytoma cell line expressed the known coreceptor for APRIL, HSPG as revealed by 10e4 mAb reactivity. Additionally, they expressed another sulfated receptor, chondroitin sulfate proteoglycan (CSPG) as revealed by CS-56 mAb reactivity (figure 3C/D, left panel). Presence of heparin, a low molecular weight HSPG, fully inhibited $APRIL_{A88}$ binding to these astrocytes, confirming that APRIL binding was strictly dependent on a sulfated receptor (figure 3C/D, middle panel). Finally, heparinase and chondroitinase treatment inhibited $APRIL_{A88}$ binding (figure 3C/D, right panel). Similar results were obtained with mouse primary astrocytes (figure 3E). Taken together, these show that APRIL is also interacting with CSPG, in addition to HSPG. The CS chain of CSPG is heterogeneous regarding the sulfation level and position on the disaccharide core unit. This is the case in the CNS, and that alters CSPG ligand binding properties [20]. In surface plasmon resonance analysis, APRIL showed a strict specificity to disulfated CS of type E but neither to disulfated type D nor to the monosulfated type A, B and C (figure 3F). The affinity of interaction of trimeric APRIL to CS type E was similar to the one measured with heparin or HSPG, in the nanomolar range.

In MS lesions, there was no reactivity with 10e4, recognizing native HSPG (data not shown). 3g10, recognizing HSPG after heparinase digestion, is believed to be of wider reactivity than 10e4. 3g10 staining revealed a similar expression of HSPG in the NAWM and inside lesions (figure 4A). CSPG as defined by CS-56 reactivity were highly present in the NAWM in cells and the extracellular matrix. In lesions, CSPG expression was less abundant, mostly confined to cells. On the contrary, CS of type E was barely present in the NAWM, but highly upregulated in cells from lesions. Costaining experiments revealed that $GFAP^+$

astrocytes from active (n=3), slowly expanding (n=2) and inactive (n=2) lesions did not express HSPG (3g10 reactivity) (figure 4B, upper panel). The non-astrocytic HSPG found in the extracellular matrix did not colocalize with secreted APRIL. In all cases, active (n=3), slowly expanding (n=2) and inactive (n=2) lesions, CSPG (CS-56 reactivity) were expressed within $GFAP^+$ astrocytes and colocalized with secreted APRIL for active and slowly expanding lesions (figure 4B, middle). We further observed expression of CS of type E within astrocytes in 2/3 active, 1/2 slowly expanding and 0/2 inactive lesions. When expressed, CS of type E colocalized with secreted APRIL in astrocytes (figure 4B, bottom panel). Taken together, our data show a selective binding of APRIL to CSPG. This binding occurs *in situ* in MS lesions at the level of reactive astrocytes. In some lesions but not all, we identified CS of type E as the APRIL binder. In MS lesions, APRIL does not bind to HSPG.

APRIL induces an IL-10 dependent anti-inflammatory response in astrocytes

Astrocytes secrete a wide array of cytokines acting on T-cell mediated autoimmune responses in the CNS [21]. We screened several of these cytokines by ELISA and CBA after stimulation of murine primary astrocytes with APRIL. *In vitro* cultured primary astrocytes are considered as non-fully resting astrocytes as judged by their constitutive expression of pro-inflammatory cytokines [22]. APRIL stimulation did not change the expression of the proinflammatory IL-6 by these *in vitro* expanded astrocytes, while it induced them to produce the anti-inflammatory IL-10, 72 hr after stimulation (figure 5A, left panel). $APRIL_{H98}$ had no effect in this experiment. We also observed a late induction of IL-10 with no change in IL-6 by $APRIL_{A88}$ in human primary astrocytes and the human astrocytoma cell line CRT (figure 5A, middle and right panel). Other cytokines reported to be produced by astrocytes including IL-2, IL-4, IL-12, IFN-γ, and TNF were not detectable at any time point over the course of the experiment. QRT-PCR analysis confirmed the late upregulation of the IL-10 mRNA in mouse

primary astrocytes 48hr after stimulation with APRIL (figure 5B). CRT astrocytoma treatment with 25 mM of NaClO3, a transient inhibitor of sulfation, reduced CSPG surface expression and APRIL binding (Figure 5C, left upper panel). HSPG decrease on CRT cells required a higher NaClO3 concentration (75 mM, data not shown). With 25 mM of NaClO3, CRT cell mortality never reached more than 15%. In this condition, IL-10 induction decreased by more than 50% after APRIL stimulation, while IL-6 was not significantly modulated (figure 5C, left bottom panel). We observed a similar inhibition of CSPG expression associated to reduced APRIL binding with 25 mM of NaClO3 treatment in human and mouse primary astrocytes (Figure 5C, middle and right panels). NaClO3 treatment also reduced by more than 50% the production of IL-10 in APRIL-treated human and mouse primary astrocytes, while leaving unchanged IL-6 secretion.

We next performed *in vitro* peptide stimulation assays with MOG-specific TCR-transgenic 2D2 $CD4^+$ T cells. In the presence of primary astrocytes treated with APRIL, 2D2 T-cell proliferation was significantly inhibited (figure 6A). Notably, IL-10 antagonism in this assay partially reverted the APRIL-mediated inhibition. Regarding IL-17A and IFN-γ, presence of APRIL-treated primary astrocytes also inhibited their production by 2D2 T cells (figure 6B). As for proliferation, addition of a blocking anti-IL10 partially reverted the APRIL-mediated inhibition. In these experiments, the effect of $APRIL_{A88}$ stimulation vanished in the absence of astrocytes (figure 6A/B right bottom panels). Hence, APRIL induces an anti-inflammatory response into astrocytes with the production of IL-10 that may protect from an autoimmune neurodegenerative insult.

EAE treatment with recombinant APRIL

We next sought to assess the effect of recombinant APRIL injection in EAE mice. We first performed a local intraspinal delivery of APRIL twice in the presymptomatic phase.

APRIL injections significantly lowered disease severity for three consecutive days (figure 7A). This route did not allow us to perform injections in the symptomatic phase due to tail paralysis in EAE mice. We then switched to the intravenous route. Nuclear imaging with Iodine-labeled recombinant APRIL showed that $APRIL_{A88}$ accumulated compared to $APRIL_{H98}$ in the spinal cord of EAE mice (figure 7B). No such level of detection was achieved in the spinal cord of healthy mice. This result may reflect leakage of the blood brain barrier, and specific retention of $APRIL_{A88}$ by CSPG upregulation in EAE lesions. Figure 7C shows that repeated intravenous injections of $APRIL_{A88}$ before and during disease significantly reduce disease severity. We observed similar reduction when $APRIL_{A88}$ treatment was started at disease onset (figure 7D). Taken together, these data shows that injection of recombinant APRIL may constitute a valuable treatment for MS.

Discussion

Antagonism of BAFF and/or APRIL with a soluble form of one of their common receptors, TACI, exacerbates neuroinflammatory diseases such as MS and ON. It could be postulated that BAFF and/or APRIL positively regulate the subset of B cells producing IL-10 and IL-35 that was shown to dampen EAE [23,24]. However, a protective role for BAFF and/or APRIL on non-immune cells present in the CNS cannot be excluded. BAFF production by astrocytes is upregulated in MS lesions, and EAE is exacerbated in *BAFF-R* KO mice [25,26]. However, a role for CNS BAFF on CNS resident cells appears unlikely, since BAFF-R expression was only reported in infiltrating immune cells [25]. We confirmed that result with the MS patients analyzed here, and extended it by showing the absence of BAFF binding and BAFF-R expression on primary astrocytes (data not shown). Hence, CNS BAFF produced by astrocytes may exert a local role but on immune infiltrating cells. Less is known regarding APRIL in MS. In the CSF of MS patients, APRIL is either slightly upregulated or unmodulated compared to control CSF from patients suffering from non-inflammatory

neurodegenerative disorders [27,28]. Tangarajh et al. reported that reactive astrocytes produced APRIL [29]. The authors used the same tissue-reactive anti-human APRIL antibody, Aprily-8. However, Aprily-8 is directed against the secreted part of APRIL, while Stalk-1 (used here) reacts with the part of the molecule that remains anchored in producing cells after processing. Hence Stalk-1 reactivity clearly detects APRIL-producing cells, while Aprily-8 reactivity may detect either APRIL-producing cells before APRIL processing or the secreted product. Our combination of Stalk-1 and Aprily-8 reactivity indicates that in MS lesions it is in fact a subset of macrophages that secretes APRIL, and reactive astrocytes selectively bind paracrine APRIL. The absence of APRIL mRNA detection in resting and activated primary astrocytes is also an evidence arguing against a production of APRIL by astrocytes. Our study also revealed that APRIL expression is variable according to the type of lesions. This is true for APRIL-producing cells. Only very few APRIL-producing macrophages were seen in initial demyelinating lesions of acute MS. APRIL-producing macrophages were also in low numbers in slowly expanding lesions. In contrast, APRIL-producing macrophages were numerous in chronic active lesions. Despite variation in the number of producing cells, reactive astrocytes homogeneously contained a high concentration of secreted APRIL. APRIL present in reactive astrocytes may originate from infiltrating macrophages but also from the blood. Indeed, the blood brain barrier is permeable to serum components in MS [30], and myeloid cells constitutively secrete APRIL in the blood [12,16,31]. These analyses demonstrate that APRIL acts locally on CNS resident astrocytes.

We did not find evidence for expression of TACI and BCMA in *in vitro* expanded astrocytes. We only found expression of the APRIL co-receptor, HSPG, and identify CSPG, a related sulfated proteoglycan, as a new APRIL binding partner in the CNS. The dual expression of HSPG and CSPG in *in vitro* cultured astrocytes is consistent with the previous study from Johnson-Green et al. [32]. *In situ* expression of proteoglycans by astrocytes is

different. HSPG are not detected, while CSPG are present in reactive astrocytes. We identified CS of type E, upregulated following different kinds of brain injury [33,34,35], as one of the binding partner of APRIL in reactive astrocytes. Astrocytes internalized paracrine APRIL. The reason for this internalization process is presently not known, warranting further, but this process is likely due to the ligand internalization property described for proteoglycans [36].

Astrocyte function in MS has long been a matter of debate [37,38]. This might be due to the important plasticity of these cells [39]. Nevertheless, astrocyte depletion has been shown by three independent research groups to exacerbate EAE, strongly arguing for a dominant protective function, at least in EAE [40,41,42]. We are showing here that APRIL induces the production of IL-10 by astrocytes. Our data complement the signaling property of APRIL in astrocytes reported by others [43]. This IL-10 induction fits well with a protective function for APRIL and astrocytes in autoimmune MS, own to the anti-inflammatory activity of this cytokine [44]. This is a likely explanation for the failure of clinical trials assessing the BAFF/APRIL antagonist, atacicept, in the autoimmune neurodegenerative disorders, MS and ON. To our knowledge, there is currently no trial in MS with an APRIL-specific antagonist, and such trial may be unwanted. By contrast, exogenous APRIL lowered severity in a mouse model of MS. Taken together, the present bed to benchside translation leads to the identification of APRIL as a potential new therapeutic compound for autoimmune neurodegenerative disorders.

Acknowledgments:

Funding: This work was supported by the University Grenoble Alpes (BH), the "institut national pour la santé et la recherche médicale" (INSERM) (BH), the association for the "aide à la recherche sur la sclérose en plaques" (ARSEP) (BH), and the agence nationale pour la recherche (ANR, program centre of excellence in neurodegeneration obtained within the

Grenoble excellence in neurodegeneration network) (BH), the Swiss national science foundation (PL) (PS, 310030_156961; 310030A_176256), and the Swiss multiple sclerosis society (PL).

Author contributions: LB, MB, NP, MCA, BM, JB, NS, GR, MT, OC, RM, MA, AB, CG, CR, CS, MH, DB, RV, HLJ, PNM, PS, HPL, JB, PL and BH contributed to the acquisition and analysis of the data performed research. PL and BH contributed to the conception and design of the study. LB, PL and BH contributed to drafting the text or preparing the figures.

Potential conflicts of interest: PS and BH report receiving a commercial research grant and speaker bureau honoraria, respectively, from Merck-Serono who is developing atacicept. Other authors declare no potential conflicts of interest.

References

1. Townsend MJ, Monroe JG, Chan AC. B-cell targeted therapies in human autoimmune diseases: an updated perspective. Immunological reviews 2010;237(1):264–83.
2. Kappos L, Hartung HP, Freedman MS, et al. Atacicept in multiple sclerosis (ATAMS): a randomised, placebo-controlled, double-blind, phase 2 trial. The Lancet. Neurology 2014;13(4):353–63.
3. Yu G, Boone T, Delaney J, et al. APRIL and TALL-I and receptors BCMA and TACI: system for regulating humoral immunity. Nature immunology 2000;1(3):252–6.
4. Sergott RC, Bennett JL, Rieckmann P, et al. ATON: results from a Phase II randomized trial of the B-cell-targeting agent atacicept in patients with optic neuritis. Journal of the neurological sciences 2015;351(1–2):174–8.
5. Kretzschmar B, Hein K, Moinfar Z, et al. Treatment with atacicept enhances neuronal cell death in a rat model of optic neuritis. Journal of neuroimmunology 2014;268(1–2):58–63.
6. Mackay F, Schneider P, Rennert P, Browning J. BAFF AND APRIL: a tutorial on B cell survival. Annual review of immunology 2003;21:231–64.
7. Hendriks J, Planelles L, de Jong-Odding J, et al. Heparan sulfate proteoglycan binding promotes APRIL-induced tumor cell proliferation. Cell death and differentiation 2005;12(6):637–48.
8. Ingold K, Zumsteg A, Tardivel A, et al. Identification of proteoglycans as the APRIL-specific binding partners. The Journal of experimental medicine 2005;201(9):1375–83.
9. Thompson JS, Bixler SA, Qian F, et al. BAFF-R, a newly identified TNF receptor that specifically interacts with BAFF. Science 2001;293(5537):2108–11.
10. Licht-Mayer S, Wimmer I, Traffehn S, et al. Cell type-specific Nrf2 expression in multiple sclerosis lesions. Acta neuropathologica 2015;130(2):263–77.
11. Varfolomeev E, Kischkel F, Martin F, et al. APRIL-deficient mice have normal immune system development. Mol. Cell. Biol. 2004;24(3):997–1006.

12. Schwaller J, Schneider P, Mhawech-Fauceglia P, et al. Neutrophil-derived APRIL concentrated in tumor lesions by proteoglycans correlates with human B-cell lymphoma aggressiveness. Blood 2007;109(1):331–8.
13. David G, Bai XM, Van der Schueren B, et al. Developmental changes in heparan sulfate expression: in situ detection with mAbs. The Journal of cell biology 1992;119(4):961–75.
14. Matthes T, McKee T, Dunand-Sauthier I, et al. Myelopoiesis dysregulation associated to sustained APRIL production in multiple myeloma-infiltrated bone marrow. Leukemia 2015;29(9):1901–8.
15. Vives RR, Lortat-Jacob H, Chroboczek J, Fender P. Heparan sulfate proteoglycan mediates the selective attachment and internalization of serotype 3 human adenovirus dodecahedron. Virology 2004;321(2):332–40.
16. Matthes T, Dunand-Sauthier I, Santiago-Raber ML, et al. Production of the plasma-cell survival factor a proliferation-inducing ligand (APRIL) peaks in myeloid precursor cells from human bone marrow. Blood 2011;118(7):1838–44.
17. Lassmann H. Review: the architecture of inflammatory demyelinating lesions: implications for studies on pathogenesis. Neuropathology and applied neurobiology 2011;37(7):698–710.
18. Frischer JM, Weigand SD, Guo Y, et al. Clinical and pathological insights into the dynamic nature of the white matter multiple sclerosis plaque. Annals of neurology 2015;78(5):710–21.
19. Mahad DJ, Trebst C, Kivisakk P, et al. Expression of chemokine receptors CCR1 and CCR5 reflects differential activation of mononuclear phagocytes in pattern II and pattern III multiple sclerosis lesions. Journal of neuropathology and experimental neurology 2004;63(3):262–73.
20. Properzi F, Asher RA, Fawcett JW. Chondroitin sulphate proteoglycans in the central nervous system: changes and synthesis after injury. Biochemical Society transactions 2003;31(2):335–6.
21. Rothhammer V, Quintana FJ. Control of autoimmune CNS inflammation by astrocytes. Seminars in immunopathology 2015;37(6):625–38.
22. Van wagoner. Interleukin-6 (IL-6) production by astrocytes: autocrine regulation by IL-6 and the soluble IL-6 receptor. J. Neurosciences 1999;19(13):5236-44.
23. Fillatreau S, Sweenie CH, McGeachy MJ, et al. B cells regulate autoimmunity by provision of IL-10. Nature immunology 2002;3(10):944–50.
24. Shen P, Roch T, Lampropoulou V, et al. IL-35-producing B cells are critical regulators of immunity during autoimmune and infectious diseases. Nature 2014;507(7492):366–70.
25. Krumbholz M, Theil D, Derfuss T, et al. BAFF is produced by astrocytes and up-regulated in multiple sclerosis lesions and primary central nervous system lymphoma. The Journal of experimental medicine 2005;201(2):195–200.
26. Kim SS, Richman DP, Zamvil SS, Agius MA. Accelerated central nervous system autoimmunity in BAFF-receptor-deficient mice. Journal of the neurological sciences 2011;306(1–2):9–15.
27. Piazza F, DiFrancesco JC, Fusco ML, et al. Cerebrospinal fluid levels of BAFF and APRIL in untreated multiple sclerosis. Journal of neuroimmunology 2010;220(1–2):104–7.
28. Wang H, Wang K, Zhong X, et al. Cerebrospinal fluid BAFF and APRIL levels in neuromyelitis optica and multiple sclerosis patients during relapse. Journal of clinical immunology 2012;32(5):1007–11.
29. Thangarajh M, Masterman T, Hillert J, et al. A proliferation-inducing ligand (APRIL) is expressed by astrocytes and is increased in multiple sclerosis. Scandinavian journal of immunology 2007;65(1):92–8.

30. Levine SM. Albumin and multiple sclerosis. BMC neurology 2016;16:47.
31. Manfroi B, McKee T, Mayol JF, et al. CXCL-8/IL-8 produced by diffuse large B-cell lymphomas recruits neutrophils expressing a proliferation inducing ligand APRIL. Cancer research 2017;77(5):1097-107.
32. Johnson-Green PC, Dow KE, Riopelle RJ. Characterization of glycosaminoglycans produced by primary astrocytes in vitro. Glia 1991;4(3):314–21.
33. Brown JM, Xia J, Zhuang B, et al. A sulfated carbohydrate epitope inhibits axon regeneration after injury. Proceedings of the National Academy of Sciences of the United States of America 2012;109(13):4768–73.
34. Gilbert RJ, McKeon RJ, Darr A, et al. CS-4,6 is differentially upregulated in glial scar and is a potent inhibitor of neurite extension. Molecular and cellular neurosciences 2005;29(4):545–58.
35. Properzi F, Carulli D, Asher RA, et al. Chondroitin 6-sulphate synthesis is up-regulated in injured CNS, induced by injury-related cytokines and enhanced in axon-growth inhibitory glia. The European journal of neuroscience 2005;21(2):378–90.
36. Belting M. Heparan sulfate proteoglycan as a plasma membrane carrier. Trends in biochemical sciences 2003;28(3):145–51.
37. Nair A, Frederick TJ, Miller SD. Astrocytes in multiple sclerosis: a product of their environment. Cellular and molecular life sciences : CMLS 2008;65(17):2702–20.
38. Williams A, Piaton G, Lubetzki C. Astrocytes--friends or foes in multiple sclerosis?. Glia 2007;55(13):1300–12.
39. Ludwin SK, Rao VT, Moore CS, et al. Astrocytes in multiple sclerosis. Mutliple sclerosis 2016;22(9):1114-24.
40. Voskuhl RR, Peterson RS, Song B, et al. Reactive astrocytes form scar-like perivascular barriers to leukocytes during adaptive immune inflammation of the CNS. The Journal of neuroscience : the official journal of the Society for Neuroscience 2009;29(37):11511–22.
41. Toft-Hansen H, Fuchtbauer L, Owens T. Inhibition of reactive astrocytosis in established experimental autoimmune encephalomyelitis favors infiltration by myeloid cells over T cells and enhances severity of disease. Glia 2011;59(1):166–76.
42. Mayo L, Trauger SA, Blain M, et al. Regulation of astrocyte activation by glycolipids drives chronic CNS inflammation. Nature medicine 2014;20(10):1147–56.
43. Deshayes F, Lapree G, Portier A, et al. Abnormal production of the TNF-homologue APRIL increases the proliferation of human malignant glioblastoma cell lines via a specific receptor. Oncogene 2004;23(17):3005–12.
44. Moore KW, O'Garra A, de Waal Malefyt R, et al. Interleukin-10. Annual review of immunology 1993;11:165–90.

Figure legends:

Figure 1: APRIL modulates the severity of EAE

A) EAE induced in WT and *APRIL* KO mice was monitored over time. The mean +/- SD for the clinical score from a pool of three independent experiments is shown. Total mouse number is also shown. B) 7 days post-immunization, total cells from spleen and lymph nodes draining (dln) the priming site were restimulated *ex vivo* with the MOG peptide IFN-γ and IL17A secretions are shown. C) The relative expression to GAPDH of April (left axis, solid bars) and MHC II (right axis, open bars) mRNA is shown for the spinal cord of EAE mice at different time points of disease evolution. A score of 1 was given to the spinal cord of healthy mice. D) APRIL mRNA expression was determined by q-PCR on the indicated FACS-sorted cells (Mi: microglia, Mac: macrophages). Results are presented as mean of 4 mice. Microglia from naive mice was given a value of 1. * $p<0,05$; *** $p<0,001$.

Figure 2: APRIL secreted by a subset of macrophages is internalized by reactive astrocytes in MS lesions.

Immunohistochemical analysis of different types of MS lesions from patients' autopsies. A) Chronic active lesion. Scale bar = 1mm. B) Acute lesion. The asterisk labels an area of profound microglia activation at the edge of the active lesion. Scale bar: 300 µm. C) Slowly expanding lesion. Scale bar: 300 µm. Inserts in A, B, C show high magnification of APRIL-producing cells and cells positive for secreted APRIL. Note that we did not use always strictly serial sections for the sake of material saving. D) Serial sections from a brain control autopsy were immunostained for APRILp. and APRILs. Scale bars = 200 µm. Pictures are representative of four cases. E) Sections from MS biopsies were costained for APRILp./CD68 (upper panel), and APRILs./GFAP (bottom panel). The costainings shown are representative of three chronic active and two slowly expanding lesions. Scale bar = 5µm**.** F) $APRIL_{A88}$-

binding astrocytoma CRT cells were incubated at 4°C or 37°C for the indicated times (left panel).. The figures show costaining for APRIL (red) and the plasma membrane (CTxB staining, green). Nuclear DAPI staining (blue) is shown on the merge pictures. An experiment with $APRIL_{H98}$ is also shown (right panel). Scale bar = 2 μm. The results are representative of four experiments.

Figure 3: CS of type E expressed on astrocytes is a new binding partner for APRIL

A) Binding of Fc-$APRIL_{A88}$, Fc-$APRIL_{H98}$ and control Fc-GITRL (CTRL) was assessed by flow cytometry on control L363 cells, human primary (huAstro), CRT astrocytoma, and mouse primary (muAstro) astrocytes. B) Expression of BCMA, TACI mRNA was determined by RT-PCR in adult mouse spleen, brain and primary astrocytes. Human primary astrocytes (C) and the CRT astrocytoma (D) were tested by flow cytometry for their reactivity with control IgM (CTRL), anti-HSPG (10e4), and anti-CSPG (CS-56) (left panel), for the binding of Fc-$APRIL_{A88}$ in the presence of heparin (middle panel), and after heparinase/chondroitinase (Chase) treatment (right panel). E) Mouse primary astrocytes were tested as in (C) for HSPG/CSPG reactivity and heparinase/chondroitinase treatment. Data are representative of at least four experiments. F) Surface plasmon resonance analysis for the binding of trimeric $APRIL_{A88}$ to the indicated coated HS and CS. Measured affinities are indicated. Results are representative of at least 3 independent experiments.

Figure 4: CS of type E expressed by reactive astrocytes is the unique binding partner for APRIL in MS lesions

A) A biopsy from a MS patient was stained for myelin (luxol fast blue), HSPG (3g10), CSPG (CS-56) and CS of type E. Pictures representative of a demyelinated lesion and the NAWM are shown. (Scale bar: 100 μm). B) The MS biopsy was also costained for APRILs

(red)/HSPG (3g10, green)/GFAP (blue) (upper panel), APRILs (red)/CSPG (CS-56, green)/GFAP (blue) (middle panel), and APRILs (red)/CS-E (green)/GFAP (blue) (lower panel). Right panels show the merge staining. Scale bar: 10 µm. The results are representative of seven MS patients.

Figure 5: APRIL induces IL-10 secretion by astrocytes

A) ELISA analysis of cytokines in supernatants of mouse, human primary astrocytes and CRT astrocytoma treated with 10 µg/ml of control Fc-GITRL (CTRL), Fc-APRIL$_{A88,}$ and Fc-APRIL$_{H98}$. IL-6 and IL-10 productions are shown. The mean of a duplicate test with min-max values is shown. B) Transcript expression of IL-10 in mouse primary astrocytes was measured by qRT-PCR. The results are expressed as the fold change relative to the expression in presence of Fc-GITRL. C) CSPG (CS56 reactivity) and APRIL$_{A88}$ binding on NaCLO3-treated CRT astrocytoma, human and mouse primary astrocytes is shown (upper panels). IL-6 and IL-10 production by NaClO3-treated cells in the presence of Fc-APRIL$_{A88}$ stimulation is shown (bottom panels). 100% represents untreated cells. Means +/- SD from three independent experiments are shown. * p<0,05; ** p<0,01; *** p<0,001; **** p<0,0001

Figure 6: IL-10 produced by APRIL-stimulated astrocytes inhibits MOG-specific responses

Total splenocytes from 2D2 TCR-transgenic mice were stimulated with the MOG peptide (3 µg/ml) in the presence of control Fc (Fc-EDA) and Fc-APRIL$_{A88}$ treated mouse primary astrocytes. The Fc-APRIL treated conditions were performed in the presence of a control mAb (cIg) and anti-mouse IL-10. In some conditions, the stimulation was performed in the absence of astrocytes. A) 2D2 T-cell proliferation is shown (upper panel). The percentages of non-dividing/dividing $CD4^+$ T cells are indicated. Mean of % +/- SD of the proliferative

response obtained in three independent experiments is also shown (bottom panel). B) IL-17A and IFN-γ production is shown (upper panel). The mean of a duplicate test with min-max values is shown. Mean of % +/- SD obtained in three independent experiments is also shown (bottom panel). 100% represents the response obtained in the presence of CTRL-treated astrocytes. * $p<0,05$; *** $p<0,001$; **** $p<0,0001$.

Figure 7: Recombinant APRIL injection lowers EAE

A) Recombinant $APRIL_{A88}$ and control EDA were injected intraspinally at day 7 and 9 post immunization. The clinical score was monitored as in figure 1A. B) The biodistribution of the indicated radiolabelled molecules is shown for the spinal cord. C/D) 50 µg of recombinant Fc-$APRIL_{A88}$ and control Fc-EDA were injected intravenously every three days for 10 days starting day-2 before disease onset (C) and at disease onset (D). Results are shown as in A). Results shown are a pool of three independent experiments. Total mouse number is shown.* $p<0,05$; *** $p<0,001$

FIGURE 1

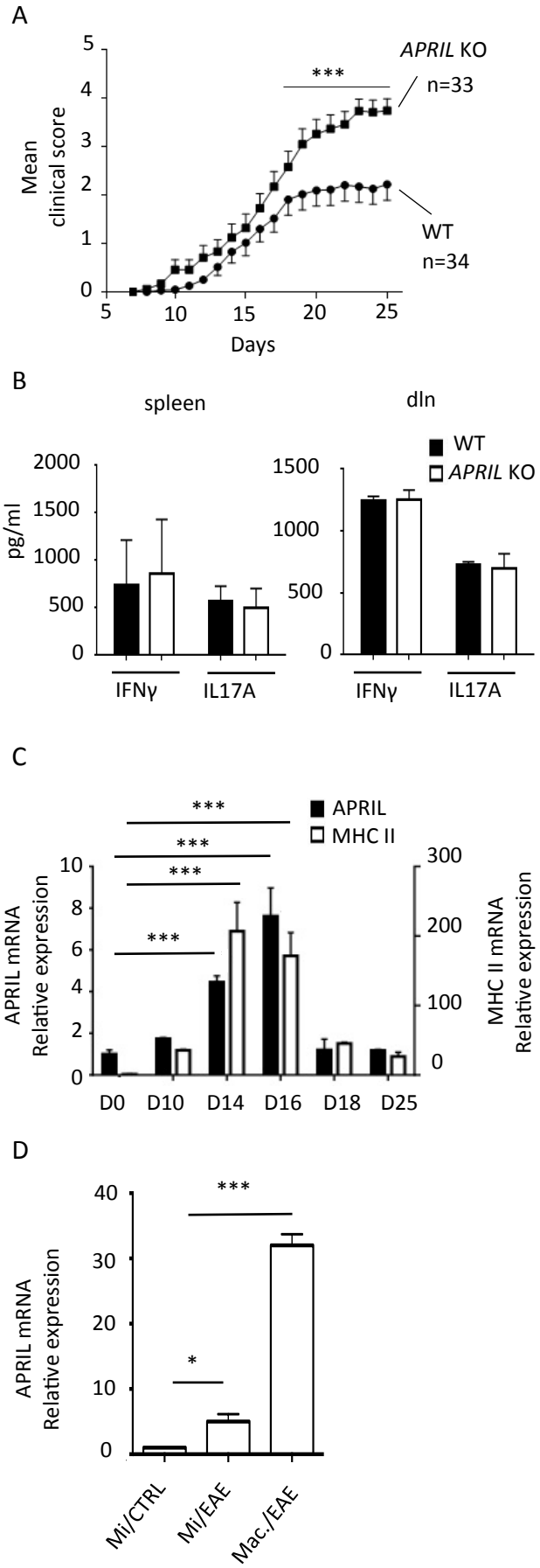
A
Mean clinical score
Days
***
APRIL KO
n=33
WT
n=34
B
spleen
dln
WT
APRIL KO
pg/ml
IFNγ
IL17A
C
APRIL
MHC II
APRIL mRNA Relative expression
MHC II mRNA Relative expression
D0
D10
D14
D16
D18
D25
D
APRIL mRNA Relative expression
Mi/CTRL
Mi/EAE
Mac./EAE

FIGURE 2

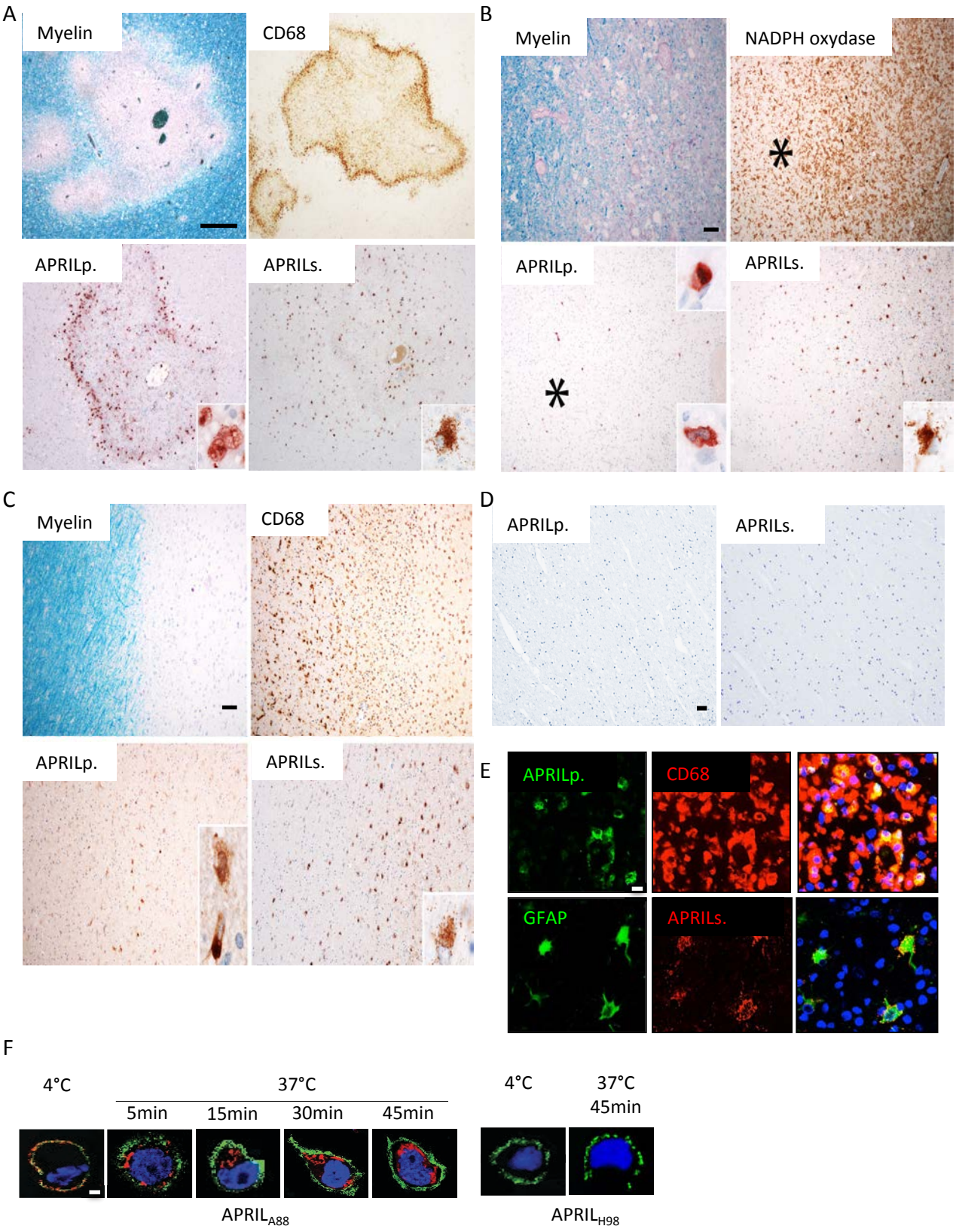
A
Myelin
CD68
APRILp.
APRILs.
B
Myelin
NADPH oxydase
APRILp.
APRILs.
C
Myelin
CD68
APRILp.
APRILs.
D
APRILp.
APRILs.
E
APRILp.
CD68
GFAP
APRILs.
F
4°C
37°C
5min
15min
30min
45min
APRIL$_{A88}$
4°C
37°C
45min
APRIL$_{H98}$

FIGURE 3

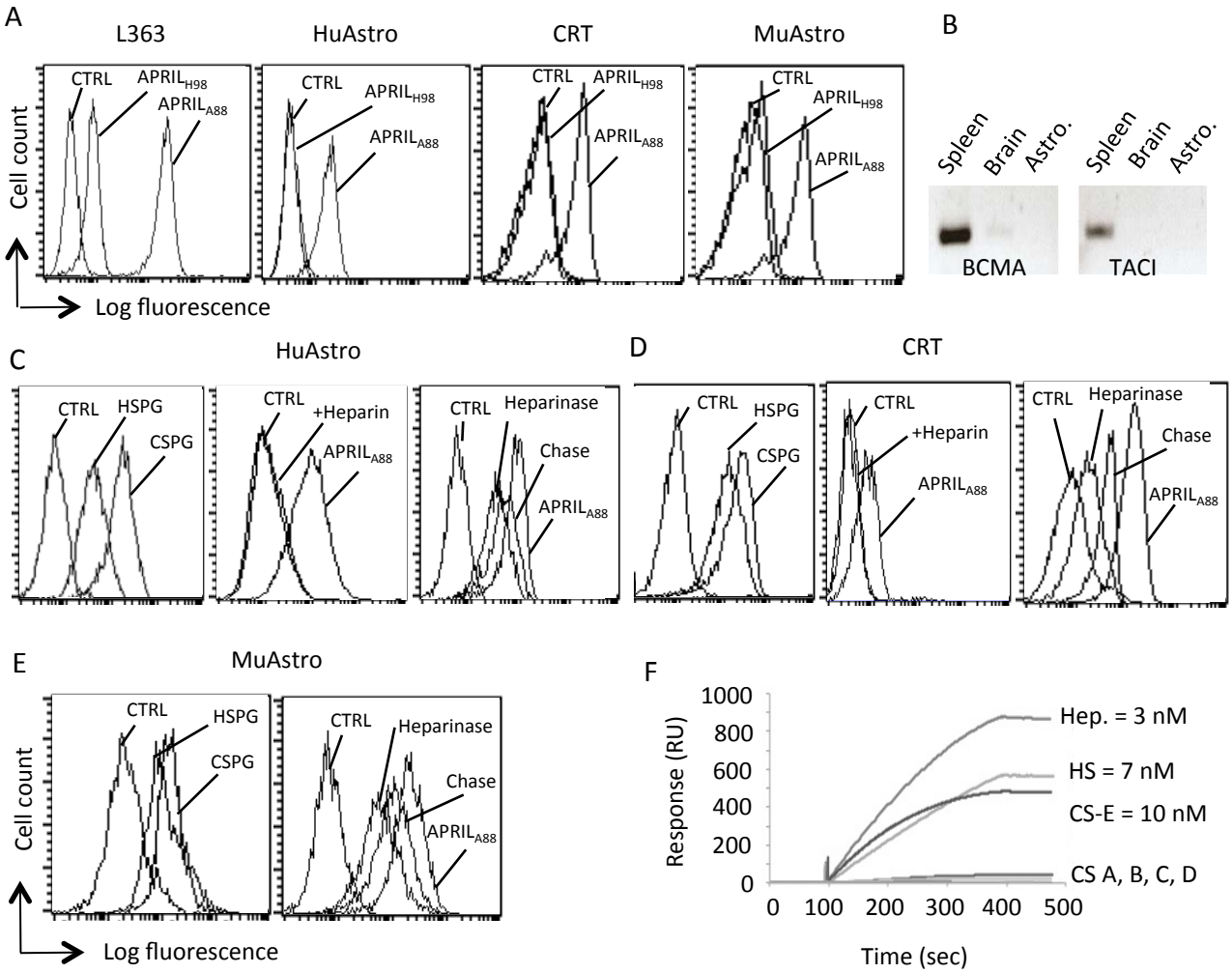
A
L363
HuAstro
CRT
MuAstro
CTRL
APRIL$_{H98}$
APRIL$_{A88}$
Cell count
Log fluorescence
B
Spleen
Brain
Astro.
BCMA
TACI
C
HuAstro
HSPG
CSPG
+Heparin
Heparinase
Chase
D
CRT
E
MuAstro
F
Response (RU)
Time (sec)
Hep. = 3 nM
HS = 7 nM
CS-E = 10 nM
CS A, B, C, D

FIGURE 4

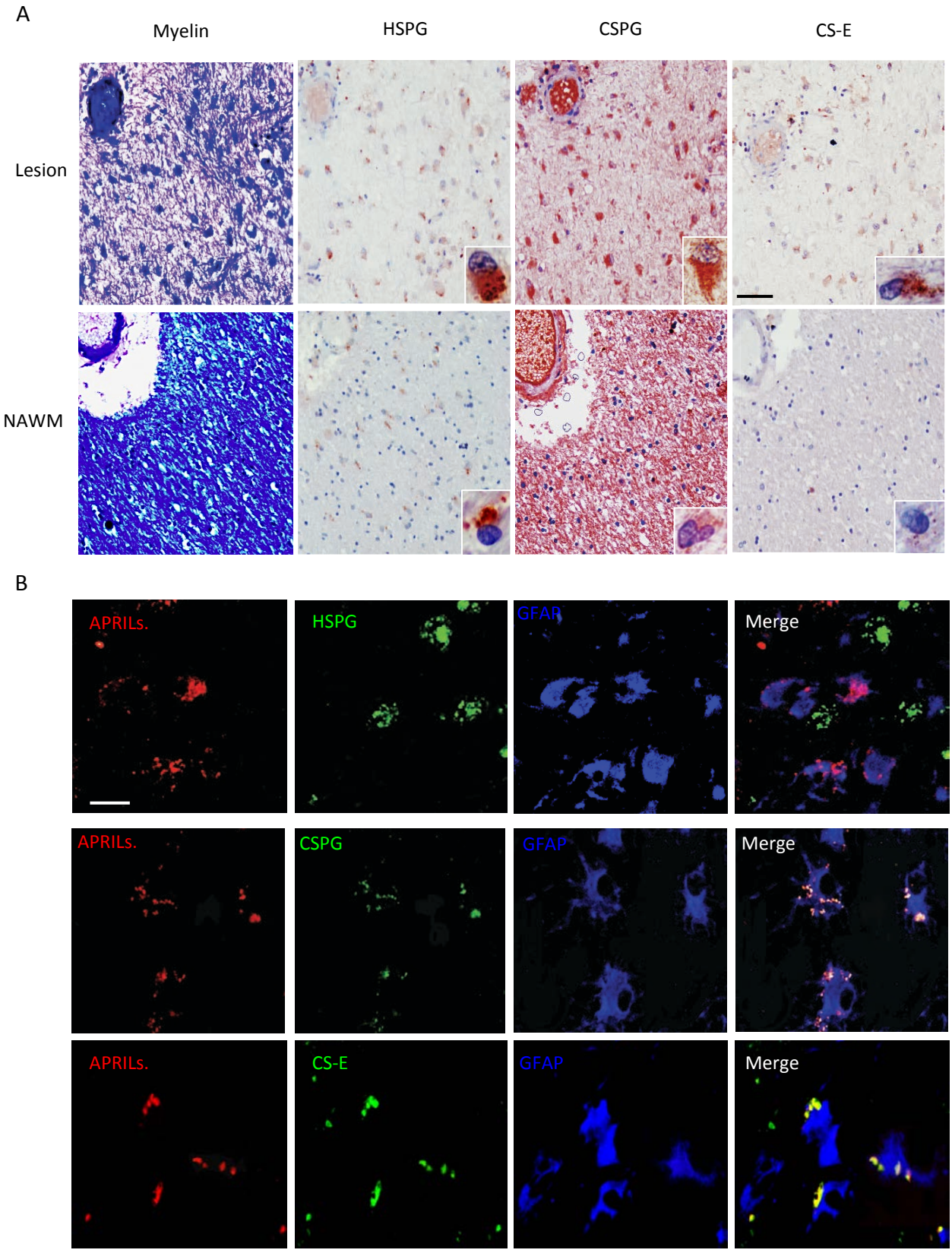
A
Myelin
HSPG
CSPG
CS-E
Lesion
NAWM
B
APRILs.
HSPG
GFAP
Merge
APRILs.
CSPG
GFAP
Merge
APRILs.
CS-E
GFAP
Merge

FIGURE 5

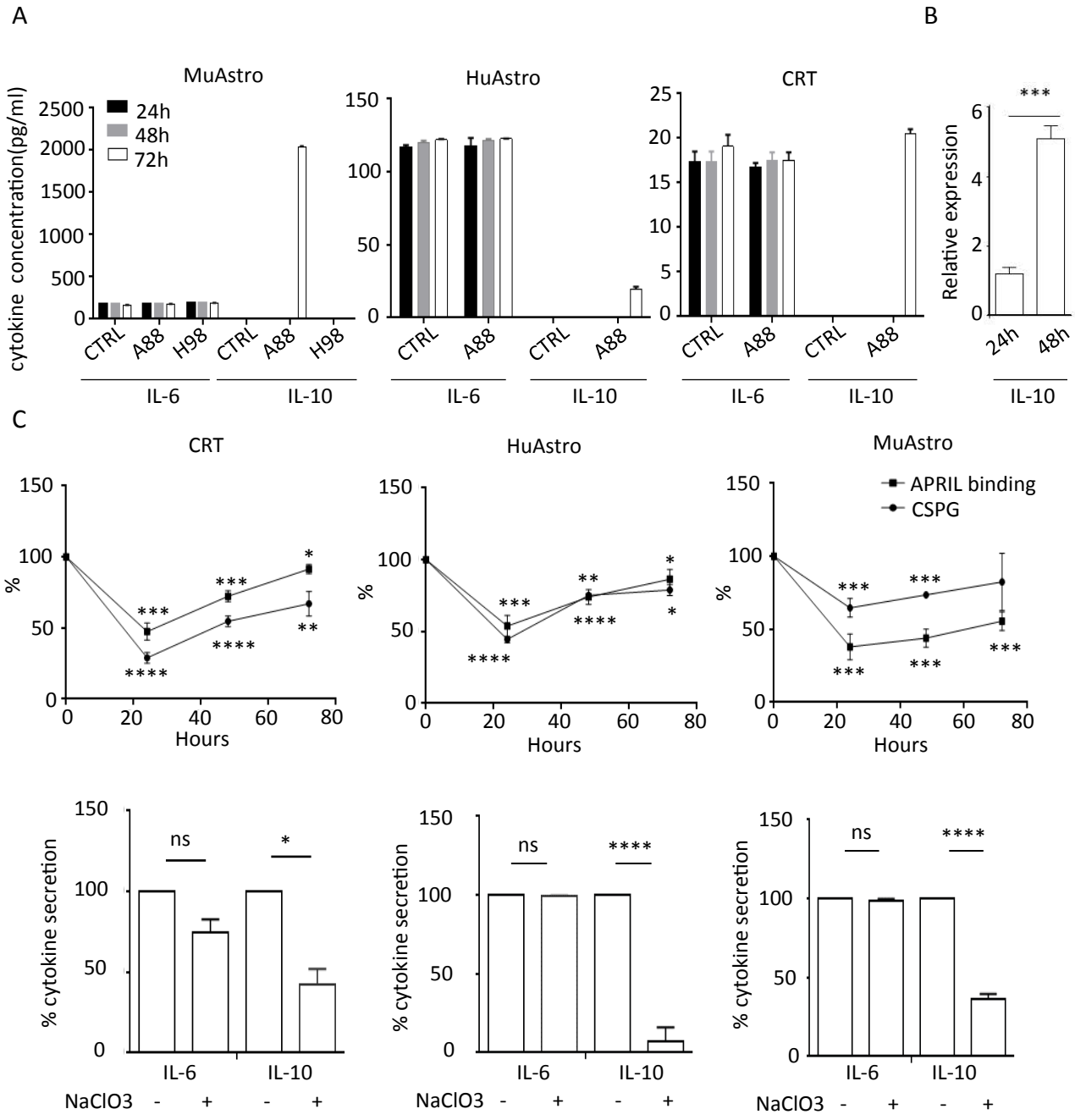
A
B
C
MuAstro
HuAstro
CRT
cytokine concentration(pg/ml)
24h
48h
72h
CTRL
A88
H98
IL-6
IL-10
Relative expression
***
24h
48h
APRIL binding
CSPG
Hours
% cytokine secretion
ns
*
****
NaClO3

FIGURE 6

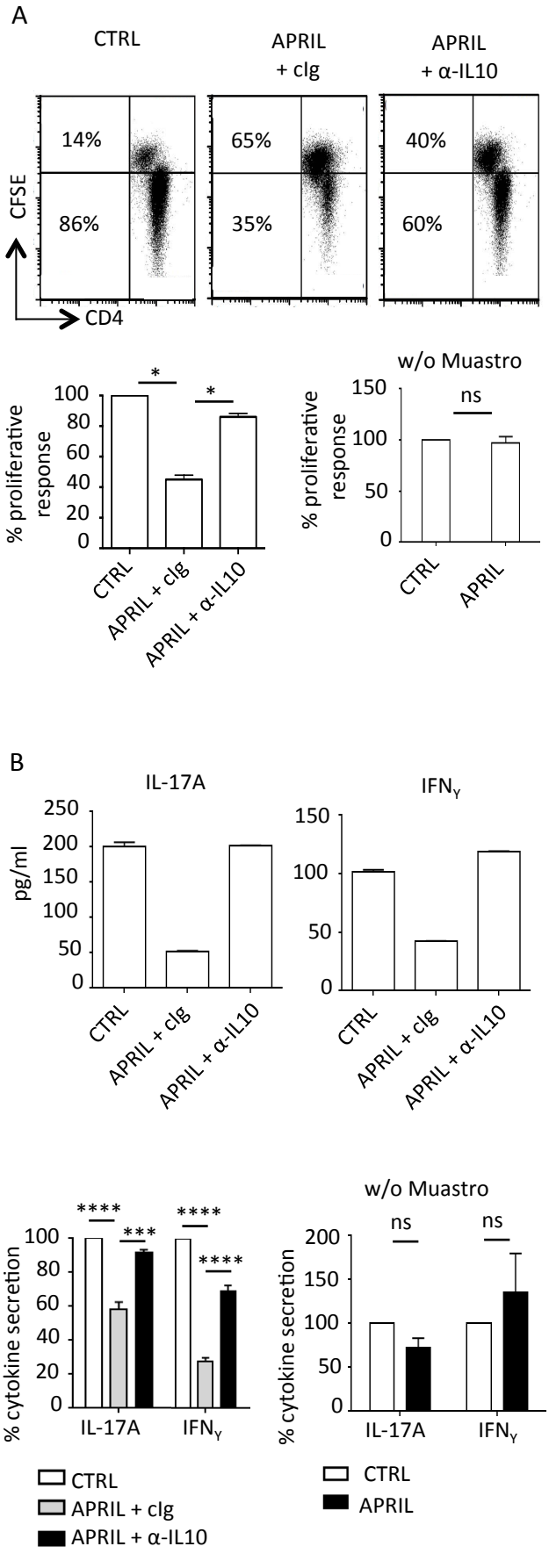
A
CTRL
APRIL + clg
APRIL + α-IL10
14%
86%
65%
35%
40%
60%
CFSE
CD4
% proliferative response
CTRL
APRIL + clg
APRIL + α-IL10
w/o Muastro
ns
APRIL
B
IL-17A
IFNγ
pg/ml
% cytokine secretion
****
***
ns
CTRL
APRIL + clg
APRIL + α-IL10
APRIL

FIGURE 7

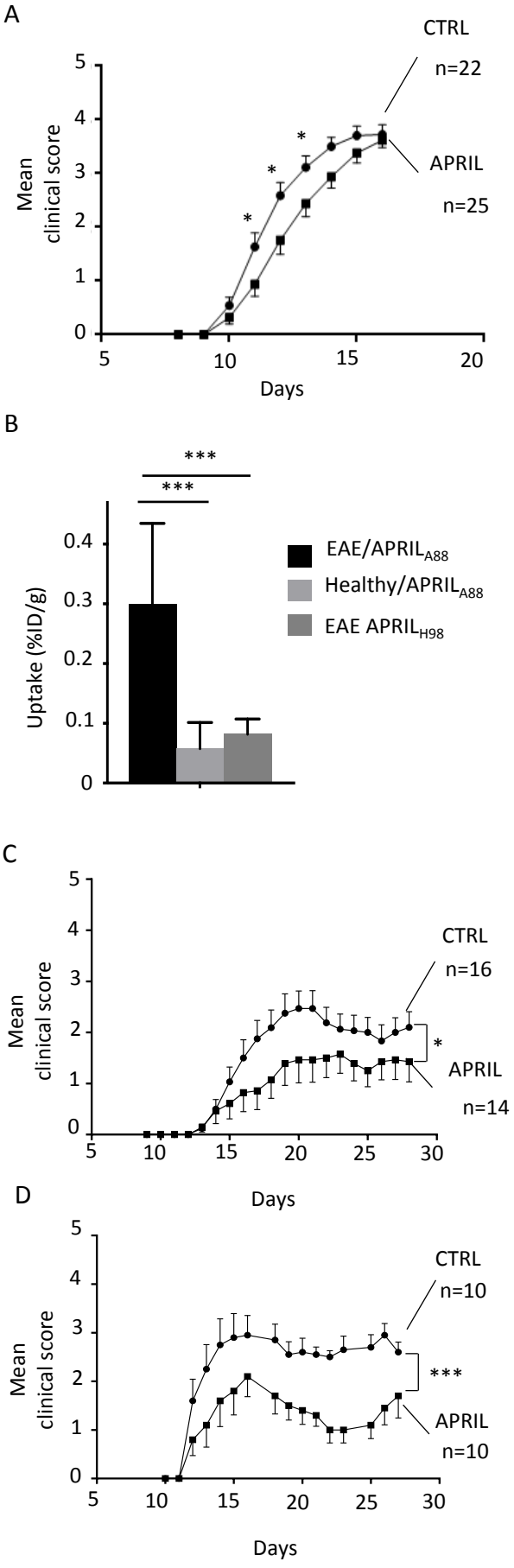
A
CTRL
n=22
APRIL
n=25
Mean clinical score
Days
B
***
***
EAE/APRIL$_{A88}$
Healthy/APRIL$_{A88}$
EAE APRIL$_{H98}$
Uptake (%ID/g)
C
CTRL
n=16
APRIL
n=14
*
Mean clinical score
Days
D
CTRL
n=10
APRIL
n=10
***
Mean clinical score
Days

TABLE 1

age	gender	lesion	MS	APRILp.				APRILs.	
				NAWM	PPWM	edge	Center	NAWM	center
35	m	Ac.	AMS	No	M	Mod. G, M	Mod. M, G	No	Astro
51	f	Ac.	AMS	No	few M	M, G	M	No	Astro
40	f	Ac.	RRMS	No	No	few G, M	few G, M	No	Astro
52	m	Chr. Act.	AMS	No	few M, G	M	few M	No	Astro
49	f	Chr. Act.	RRMS	No	few G, M	M	few M	No	Astro
41	m	Chr. Act.	SPMS	No	few M, G	weak M	few M	No	Astro
46	f	Chr. Act.	SPMS	No	Mod G, M	Mod. G, M	few M	No	Astro
61	f	SE	SPMS	No	few G, M	few G, M	few M	No	Astro
67	m	SE	PPMS	No	few G. M	Mod. M	few M	No	Astro
56	m	SE	SPMS	No	few G. M	few G, M	M	No	Astro
53	m	Inact.	PPMS	No	M	M	M	No	Astro
71	f	Inact.	PPMS	No	M	M	M	No	Astro
34	m	Inact.	PPMS	No	few G, M	few M	M	No	Astro
62	f	Inact.	SPMS	No	M	M	M	No	Astro
77	f	Inact.	PPMS	No	No	few G, M	few M	No	Astro

M = male, f = female
Ac.= acute, Chr. Act. = chronic active, SE = slowly expanding, Inact. = inactive
AMS = active multiple sclerosis
NAWM = normal appearing white matter, PPWM = periplaque white matter
G = granulocyte, M = monocyte/macrophage, Astro = astrocytes
Mod. = moderate